

*J. Yang, C. Ran, et al, Atom-economical design of PET tracer for imaging  $\alpha_v\beta_3$  integrin via utilizing three-in-one function of  $^{64}\text{Copper}$*

**Atom-economical design of PET tracer for imaging  $\alpha_v\beta_3$  integrin via utilizing three-in-one function of  $^{64}\text{Copper}$**

Jing Yang<sup>1,2,6</sup>, Jian Yang<sup>1,3,6</sup>, Huan Wang<sup>1</sup>, Junfeng Wang<sup>4</sup>, Jianping Xiong<sup>5</sup>, Chunhua Qiao<sup>2</sup>, and Chongzhao Ran<sup>1\*</sup>

<sup>1</sup>Athinoula A. Martinos Center for Biomedical Imaging, Massachusetts General Hospital and Harvard Medical School, Boston, MA, 02129; <sup>2</sup>College of Pharmaceutical Sciences, Soochow University, Suzhou, 215006, China; <sup>3</sup>School of Pharmacy, China Pharmaceutical University, Nanjing, 210009, China; <sup>4</sup>Gorden Center for Medical Imaging, Massachusetts General Hospital and Harvard Medical School, Boston, MA, 02129; <sup>5</sup>Program in Structural Biology, Nephrology Division, Massachusetts General Hospital and Harvard Medical School, Boston, MA, 02129; <sup>6</sup>These authors contributed equally to this work.

## **Contents**

<b>Materials and Methods .....</b>	<b>Page 3-7</b>
<b>Supplemental Figures .....</b>	<b>Page 8-12</b>
<i>SI Fig.1.....</i>	<i>Page 8</i>
<i>SI Fig.2.....</i>	<i>Page 8</i>
<i>SI Fig.3.....</i>	<i>Page 9</i>
<i>SI Fig.4.....</i>	<i>Page 9</i>
<i>SI Fig.5.....</i>	<i>Page 10</i>
<i>SI Fig.6.....</i>	<i>Page 10</i>
<i>SI Fig.7.....</i>	<i>Page 11</i>
<i>SI Fig.8.....</i>	<i>Page 11</i>
<i>SI Fig.9.....</i>	<i>Page 12</i>
<i>SI Table 1.....</i>	<i>Page 12</i>
<i>SI Table 2.....</i>	<i>Page 12</i>

## **Materials and methods**

All of the chemicals were purchased from commercial vendors and used without further purification. GHRGDHG, GHK and other peptides were purchased from GenScript (Piscataway, NJ). Cilengitide (Cat. No. SML 1594) was purchased from Sigma-Aldrich. Cyclo(-RGDfK) (Cat. No. AS-61111) was purchased from Anaspec. Human vitronectin (Cat. No. CC080) and human fibronectin (Cat. No. FC010) were purchased from Millipore Sigma. Human integrin  $\alpha_v\beta_3$  (Cat. No. 3050-AV-050) and Human integrin  $\alpha_5\beta_1$  (Cat. No. 3230-A5-050) were purchased from R&D systems. Mouse anti-human CD51/61 (Cat. No. 550037) or mouse anti-human CD49e (Cat. No. 555651) were purchased from BD Biosciences. Goat anti-mouse IgG Antibody, HRP conjugate (Cat. No. 12-349) was purchased from Millipore Sigma. 1-Step Ultra TMB-ELISA (Cat. No. 34028) was purchased from Thermo Scientific.  $^{64}\text{CuCl}_2$  was produced by Cyclotron of University of Wisconsin at Madison.  $^1\text{H}$  and  $^{13}\text{C}$  NMR spectra were recorded at 500 and 125 MHz, respectively. Fluorescence measurements were carried out using an F-4500 fluorescence spectrophotometer (Hitachi). Micro-PET scans were performed using a G4 scanner (Perkin Elmer). Nude mice (nu/nu COX7) were purchased from Massachusetts General Hospital. All animal experiments were approved by the Institutional Animal Care and Use Committee at Massachusetts General Hospital.

**Cu-Cyclo-RGD preparation:** 20 mg of GHRGDHG free ligand was dissolved in 0.5 mL of water, and 1 equiv. of  $\text{CuSO}_4$  stock solution was added to ligand. Then carefully adjusted pH to neutral by addition of 0.1M NaOH till the blue color solution turned to purple. Gravity filtration was done on the solution through a pre-equilibrated Chelex® 100 column to eliminate any dissolved free Cu species. Quality of the complex was checked by HPLC-MS and quantity of the complex was determined by ICP-MS. Then the solution was freeze-dried into powder for further test/use.

**HPLC-MS condition:** Liquid chromatography-mass spectrometry (LC-MS) was performed using an Agilent 1260 Series apparatus with an LC/MSD trap and Daly conversion dynode detector with UV detection at 220, 254, and 280 nm. The reverse phase high pressure liquid chromatography (RP-HPLC) methods used on this system is as follow:

*J. Yang, C. Ran, et al, Atom-economical design of PET tracer for imaging  $\alpha_v\beta_3$  integrin via utilizing three-in-one function of  $^{64}\text{Copper}$*

RESTEK Ultra Aqueous C18 Column (150 × 4.6 mm 100 Å); eluent A: 10 mM ammonium acetate in water, eluent B: 90 % MeCN and 10 % 10 mM ammonium acetate in water; gradient: 5 % D from 0-1 min, 5 to 95 % D from 1-11 min, 95 % D from 11-13 min, 95 to 5% D from 13-14 min, 5% D from 14-15 min; flow rate at 0.7 mL/min.

**ICP-MS:** Metal concentrations were determined using an Agilent 8800-QQQ ICP-MS system. All samples were diluted with 0.1 % Triton X-100 in 5 % nitric acid. A linear calibration curve for each metal ranging from 0.1 ppb to 200 ppb was generated daily for the quantification.

**ITC test:** Isothermal titration calorimetry measurements were performed at a constant atmospheric pressure and a constant temperature of 25°C, using an ultrasensitive VP-ITC micro calorimeter (Microcal, Northampton, USA).  $\text{CuCl}_2$  and peptide solutions were prepared in 80 mM HEPES buffer. All solutions were degassed for at least 5 minutes right before each experiment. The heat of dilution was determined under identical conditions by injecting the metal ion solution into the cell containing only the sample solution. The titration data were analyzed using the Origin for ITC. The binding of Cu(II) to GHRGDHG and GHK was studied analogously to the reference reported GHK experiments<sup>[1]</sup>. HEPES buffer (80 mM, pH7.4) was used as the medium.  $\text{CuCl}_2$  (0.7 mM), stabilized with 2.8 mM Gly, was injected into the peptide solution (0.08 mM). For each experiment, 30 injections of 10  $\mu\text{L}$  titrant were performed with an interval of 300 seconds.

**Stability test of Cu-Cyclo-RGD:** This test was conducted under physiological pH conditions (10 mM PBS, pH 7.4), at 37°C. GHRGDHG and Cu-Cyclo-RGD (15 mM, 10  $\mu\text{L}$ ) were incubated with 50  $\mu\text{L}$  PBS (10 mM, pH = 7.4), fresh prepared 60% rat plasma and 500 mg/mL BSA for 2h. Two volumes of acetonitrile (120  $\mu\text{L}$ ) were added and the mixture was centrifuged (4°C, 10,000 g, 10 min) and the supernatant was analyzed by LC-MS.

**Integrin Binding Assay:** The activity and selectivity of integrin ligands were determined by a solid-phase binding assay according to the previously reported protocol<sup>[2, 3]</sup> using coated extracellular matrix proteins and soluble integrins. Cilengitide was used as internal

standard. Corning 96 well EIA/RIA assay microplates were coated overnight at 4°C with the human vitronectin 1.0  $\mu\text{g/mL}$  or human fibronectin 0.5  $\mu\text{g/mL}$  (100  $\mu\text{L}$  per well) in carbonate buffer (15 mM  $\text{Na}_2\text{CO}_3$ , 35 mM  $\text{NaHCO}_3$ , pH 9.6). Each well was then washed with PBS-T-buffer (phosphate-buffered saline/Tween20, 137 mM NaCl, 2.7 mM KCl, 10 mM  $\text{Na}_2\text{HPO}_4$ , 2 mM  $\text{KH}_2\text{PO}_4$ , 0.01% Tween20, pH 7.4; 3X200  $\mu\text{L}$ ) and blocked for 1 h at room temperature with TS-B-buffer (Tris-saline/BSA buffer; 150  $\mu\text{L}/\text{well}$ ; 20 mM Tris-HCl, 150 mM NaCl, 1 mM  $\text{CaCl}_2$ , 1 mM  $\text{MgCl}_2$ , 1 mM  $\text{MnCl}_2$ , pH 7.5, 1% BSA). In the meantime, a dilution series of the compound and internal standard is prepared in an extra plate, starting from 20  $\mu\text{M}$  to 0.256 nM in 1:5 dilution steps. After washing the assay plate three times with PBS-T (200  $\mu\text{L}$ ), 50  $\mu\text{L}$  of the dilution series were transferred to each well from B–G. Well A was filled with 100  $\mu\text{L}$  TSB-solution (blank) and well H was filled with 50  $\mu\text{L}$  TS-B-buffer. 50  $\mu\text{L}$  of a solution of human integrin  $\alpha_v\beta_3$  4.0  $\mu\text{g/mL}$  or  $\alpha_5\beta_1$  2.0  $\mu\text{g/mL}$  in TS-B-buffer was transferred to wells H–B and incubated for 1h at rt. The plate was washed three times with PBS-T buffer, and then primary antibody mouse anti-human CD51/61 4.0  $\mu\text{g/mL}$  or mouse anti-human CD49e 1.0  $\mu\text{g/mL}$  (100  $\mu\text{L}/\text{well}$ ) was added to the plate. After incubation for 1h at rt, the plate was washed three times with PBS-T. Then, secondary peroxidase-labeled antibody (2.0  $\mu\text{g/mL}$ , 100 $\mu\text{L}/\text{well}$ ) was added to the plate and incubated for 1h at rt. After washing the plate three times with PBS-T, the plate was developed by quick addition of 1-Step Ultra TMB solution and incubated for 5 min at rt in the dark. The reaction was stopped with 3 M  $\text{H}_2\text{SO}_4$  (50  $\mu\text{L}/\text{well}$ ), and the absorbance was measured at 450 nm with a plate reader (Spectra Max Plus 384, Molecular devices). The IC50 values were calculated by nonlinear regression analysis with equation  $\log(\text{inhibitor})$  vs. response using the Prism 8. Each data point was a result of the average of triplicate wells.

**Molecular Modeling:** The RGD loop structure of fibronectin type III domain 10 bound to integrin  $\alpha\text{V}\beta_3$  (PDBid: 4mmx)<sup>[4]</sup> was used to model peptide GHRGDHG by mutating corresponding residues to the desired ones using Coot<sup>[5]</sup>. A copper ion was then added into the resulting peptide model. Manual adjustment was only applied to Gly and His residues flanking the RGD motif to maintain the bond length of both Cu-O and Cu-N to about 2Å<sup>[6]</sup>. The resulting model was then regularized to obtain good geometry on the final

model.

**Cell uptake:** About  $8 \times 10^4$  cells (U87 and MCF-7) were seeded in 24 well plates and allowed to attach for 24 h. Cells were then exposed to 0.1-30  $\mu\text{L}$  of  $^{64}\text{Cu}$ -Cyclo-RGD complex (10  $\mu\text{L}$  = 75  $\mu\text{Ci}$ ) and incubated for 2 h. The culture medium was removed and cells were washed three times with PBS. Then 300  $\mu\text{L}$  of trypsin was added to each well and the cells were collected. The cell bound radioactivity was counted using an auto gamma scintillation well counter (Packard CobraII). The IC50 values were calculated by nonlinear regression analysis using the GraphPad Prism fitting program. Each data point was a result of the average of triplicate wells.

**Animal model:** All animal experimental procedures were approved by the Institutional Animal Care and Use Committee (IACUC) at Massachusetts General Hospital, and carried out in accordance with the approved guidelines. Two-month nude mice were subcutaneously implanted with  $3 \times 10^6$  U87MG cells in the right shoulder. The in vivo imaging was performed at 3 weeks after the tumor implantation.

**Small-Animal microPET imaging:** Micro-PET scans were performed using a G4 scanner (Perkin Elmer). The U87MG tumor-bearing mice ( $n = 3$ ) were first anesthetized with isoflurane and then each was intravenously injected with 20  $\mu\text{Ci}$  Peptide- $^{64}\text{Cu}$  complex. A dynamic imaging of 60-minutes was first conducted, and then 30-minutes static scans were acquired at desired time points. 3D ROIs were drawn over the tumor and organs (decay-corrected). The radioactivity concentration within the tumor, muscle, liver, kidney and bladder were obtained from the mean values of the multiple ROIs and then converted to %ID/cc. For the blocking experiment, [c(RGDfK)]<sub>2</sub> or GHRGDHG (1.0 mg/kg) were injected 30 min before the injection of 20  $\mu\text{Ci}$  peptide- $^{64}\text{Cu}$  complex.

**Bio-distribution studies:** U87 xenograft-bearing nude mice ( $n = 3$ ) were injected with  $^{64}\text{Cu}$ -Cyclo-RGD (10  $\mu\text{Ci}$ ) through a tail vein catheter. The animals then were sacrificed at 4 h after injection and blood, tumor and major organs were harvested, weighed, and their corresponding activities were counted using the auto gamma scintillation well counter (Packard CobraII). The results were reported in %ID/g, which were calculated by dividing

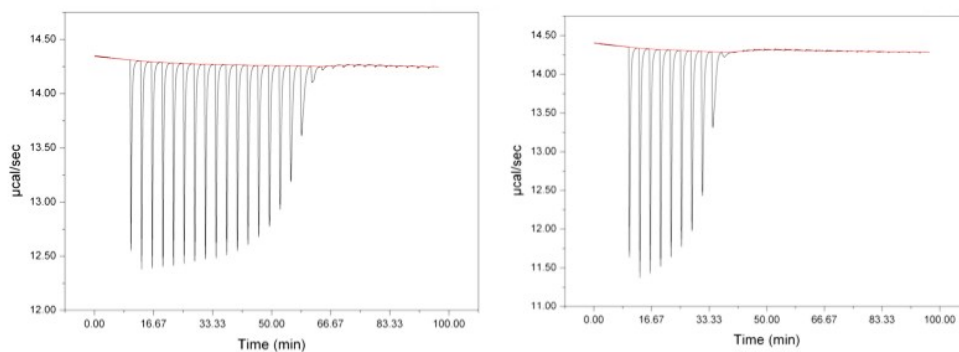
*J. Yang, C. Ran, et al, Atom-economical design of PET tracer for imaging  $\alpha_v\beta_3$  integrin via utilizing three-in-one function of  $^{64}\text{Cu}$*

the counts of  $^{64}\text{Cu}$  per gram of tissue by the total counts of the injected dose.

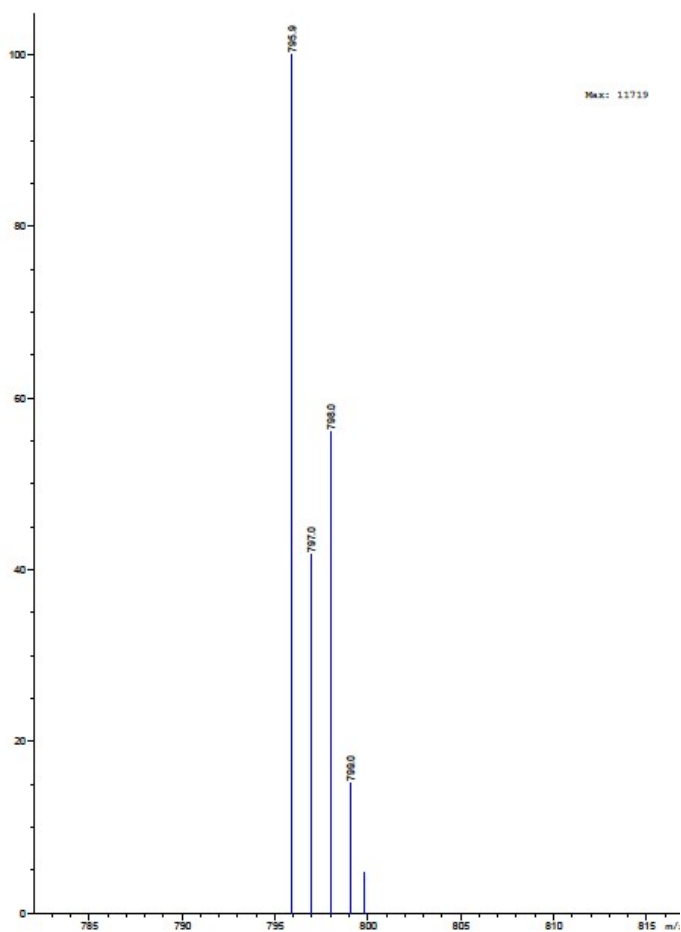
### Reference:

- [1] Trapaidze, A.; Hureau, C.; Bal, W.; Winterhalter, M.; Faller, P., Thermodynamic study of  $\text{Cu}^{2+}$  binding to the DAHK and GHK peptides by isothermal titration calorimetry (ITC) with the weaker competitor glycine. *Journal of biological inorganic chemistry : JBIC : a publication of the Society of Biological Inorganic Chemistry*. **2012**, *17* (1), 37-47.
- [2] Frank, A. O.; Otto, E.; Mas-Moruno, C.; Schiller, H. B.; Marinelli, L.; Cosconati, S.; Bochen, A.; Vossmeier, D.; Zahn, G.; Stragies, R.; Novellino, E.; Kessler, H., Conformational Control of Integrin-Subtype Selectivity in *iso*DGR Peptide Motifs: A Biological Switch. *Angew. Chem. Int. Ed.* **2010**, *49*, 9278– 9281.
- [3] Kapp, T. G.; Rechenmacher, F.; Neubauer, F.; Maltsev, O. V.; Cavalcanti-Adam, E. A.; Zarka, R.; Reuning, U.; Notni, J.; Wester, H.; Mas-Moruno, C.; Spatz, J.; Geiger, B.; Kessler, H., A Comprehensive Evaluation of the Activity and Selectivity Profile of Ligands for RGD-binding Integrins. *Sci. Rep.* **2017**, *7*, 39805.
- [4] Van Agthoven, J. F., et al., Structural basis for pure antagonism of integrin  $\alpha_v\beta_3$  by a high-affinity form of fibronectin. *Nat Struct Mol Biol*, **2014**, *21*(4), 383-8.
- [5] Emsley, P., et al., Features and development of Coot. *Acta Crystallogr D Biol Crystallogr*, **2010**, *66*(Pt 4), 486-501.
- [6] Harding, M. M., Small revisions to predicted distances around metal sites in proteins. *Acta Crystallogr D Biol Crystallogr*, **2006**, *62*(Pt 6), 678-82.
- [7] Chen, X.Y.; Park, R.; Tohme, M.; Shahinian, A. H.; Bading, J. R.; Conti, P.S., MicroPET and autoradiographic imaging of breast cancer  $\alpha_v$ -integrin expression using  $^{18}\text{F}$ - and  $^{64}\text{Cu}$ -Labeled RGD Peptide, *Bioconjug Chem.* **2004**, *15*(1): 41-49.
- [8] Wei, L. H.; Ye, Y.P.; Wadas, T. J.; Lewis, J. S.; Welch, M. J.; Achilefu, S.; Anderson, C.J.,  $^{64}\text{Cu}$ -labeled CB-TE2A and Sar conjugated RGD peptide analogs for targeting angiogenesis: Comparison of their biological activity. *Nucl Med Biol.* **2009**, *36*(3): 277-285.

### Supplemental Figures



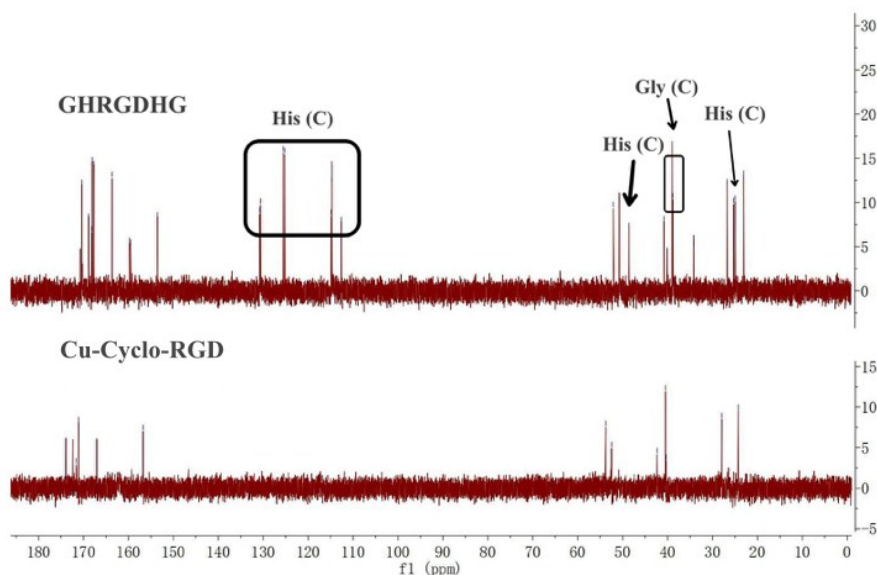
**SI Fig. 1** ITC measurement of GHK-Cu (left) and Cu-Cyclo-RGD (right).



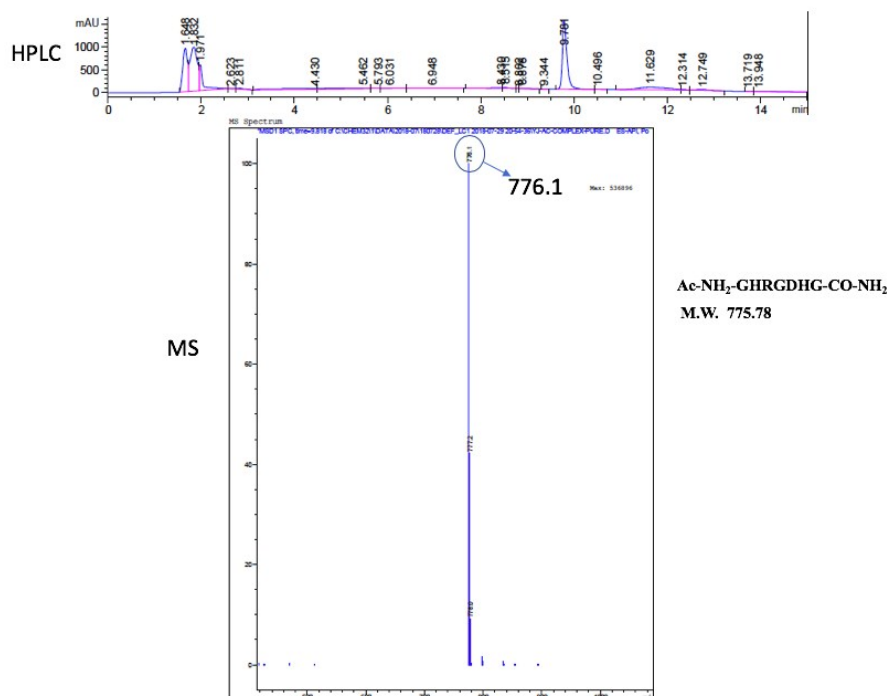
**SI Fig. 2** MS of the complex Cu-Cyclo-RGD.



*J. Yang, C. Ran, et al, Atom-economical design of PET tracer for imaging  $\alpha_v\beta_3$  integrin via utilizing three-in-one function of  $^{64}\text{Cu}$*

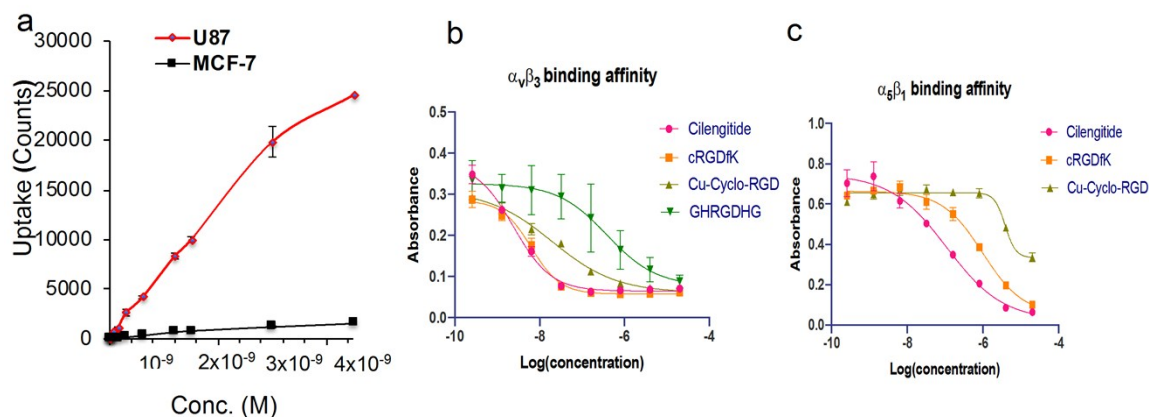


**SI Fig. 3**  $^{13}\text{C}$  NMR spectra of the linear GHRGDHG and Cu-Cyclo-RGD. The changes before and after the Cu-coordination are highlighted.

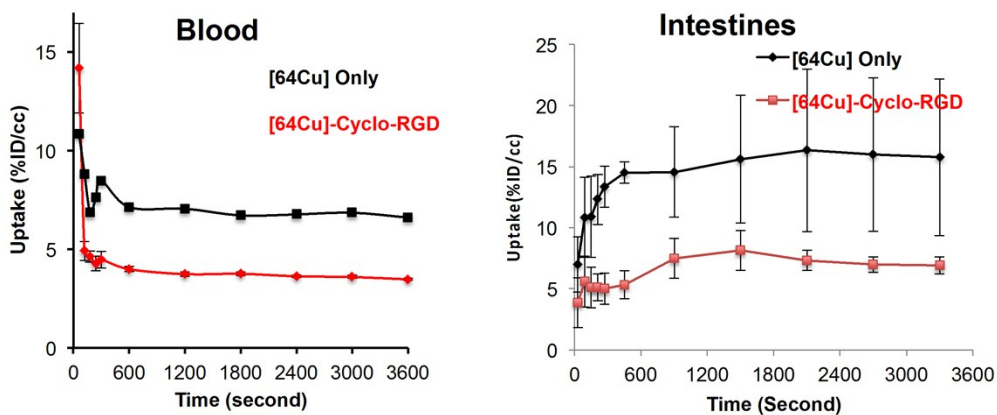


**SI Fig. 4** LC-MS of the Peptide-Cu complex after incubation of  $\text{Ac-NH}_2\text{-GHRGDHG-CO-NH}_2$  and  $\text{CuSO}_4$ .

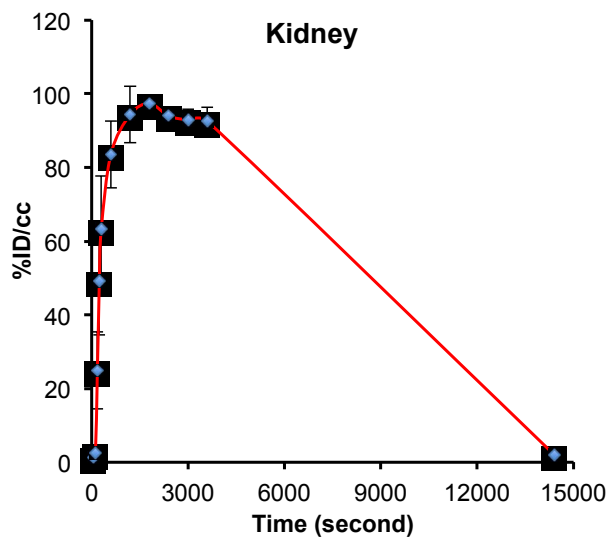
*J. Yang, C. Ran, et al, Atom-economical design of PET tracer for imaging  $\alpha_v\beta_3$  integrin via utilizing three-in-one function of  $^{64}\text{Cu}$  Copper*



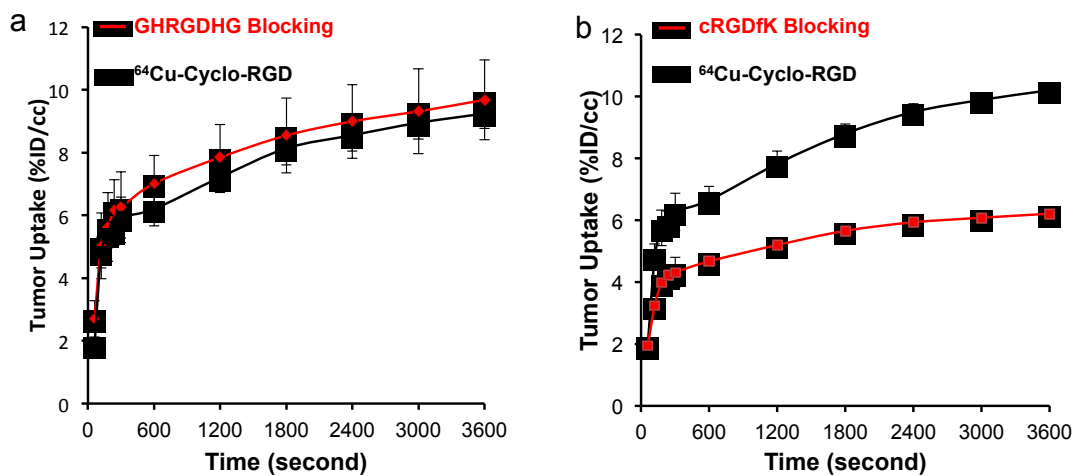
**SI Fig. 5** a) Cell uptake testing of  $^{64}\text{Cu}$ -Cyclo-RGD in U87 and MCF-7. b) IC<sub>50</sub> of different RGD tracers for  $\alpha_v\beta_3$  integrin. c) IC<sub>50</sub> of different RGD tracers for  $\alpha_5\beta_1$  integrin.



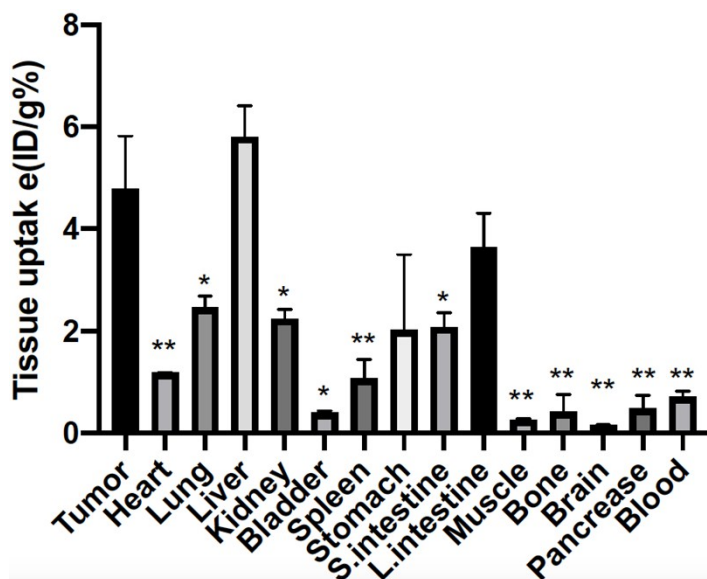
**SI Fig. 6** Comparison of blood and intestine clearance/accumulation of  $^{64}\text{CuCl}_2$  and  $^{64}\text{Cu}$ -Cyclo-RGD.



**SI Fig. 7** Clearance of  $^{64}\text{Cu}$ -Cyclo-RGD from kidney in U87 tumor bearing mice.



**SI Fig. 8** Blocking studies with linear GHRGDHG and cRGDfK (n=3). a) TAC of blocking with linear GHRGDHG, and b) TAC of blocking with cRGDfK.



**SI Fig. 9** Bio-distribution of  $^{64}\text{Cu}$ -Cyclo-RGD in nude mice (n=3).

**SI Table 1.** The stability of GHRGDHG and Cu-Cyclo-RGD in different conditions

Conditions	Percentage of compound remaining after 2 h	
	GHRGDHG	Cu-Cyclo-RGD
PBS	99.86±0.03	82.70±8.50
60% Plasma	1.36±0.15	74.38±3.78
BSA	33.93±1.96	90.98±2.58

**SI Table 2.** Comparison of in vivo data for  $^{64}\text{Cu}$ -Cyclo-RGD and other reported cyclo-RGD tracers.

	$^{64}\text{Cu}$ -Cyclo-RGD	$^{64}\text{Cu}$ -DOTA-RGD [2]	$^{64}\text{Cu}$ -diansar-c(RGDfD) [3]	$^{64}\text{Cu}$ -CB-TE2A-c(RGDyK) [3]
Tumor/Liver	1.12 ± 0.12	0.51 ± 0.09	0.24 ± 0.04	0.86 ± 0.29
Tumor/Muscle	19.18 ± 1.76	6.30 ± 1.28	4.0 ± 0.29	3.53 ± 0.80